Advances in Computational Sciences and Technology
ISSN 0973-6107 Volume 11, Number 2 (2018) pp. 85-104

http://www.ripublication.com

Two Dimensional Finite Element Simulation of Calcium Diffusion in Cardiac Myocytes Involving Pump, Leak and Excess Buffers

Kunal Pathak

Institute of Technology, Nirma University, Ahmedabad, Gujarat, India.

Abstract

The expansion and contraction of myocytes is responsible for pumping of the blood in heart required for circulation of blood in the blood vessels in human body. This expansion and contraction of myocytes depends on calcium signaling in myocytes which is achieved by diffusion of calcium, out flux of calcium through pump, influx of calcium through leak and buffering mechanism in the cardiac myocytes. Here a two dimensional finite element simulation of calcium regulation mechanism in cardiac myocytes is developed. Various processes like calcium diffusion, influx due to leak, out flux due to pump and excess buffer concentration are incorporated here. Boundary conditions have been framed according to physiology of the cell. The coaxial circular elements have been used to solve reaction diffusion equation using finite element method. The numerical results have been used to understand the effect of excess buffers, pump and leak on calcium distribution in myocytes.

Keywords: Cardiac myocytes, reaction diffusion equation, excess buffer, SERCA pump, leak, finite element method

1. INTRODUCTION

The heart consists of cardiac myocytes, which are primary cells responsible for the functioning of heart. The expansion and contraction of myocytes takes place in the heart to pump the blood into arties and regulate the blood circulation in the blood vessels. The expansion and contraction of myocytes depends on regulation of calcium distribution in the myocytes. The process of regulation of expansion and contraction of myocytes and calcium distribution in myocytes are still not well understood. It is necessary to understand calcium distribution in myocyte to understand the function of heart. The specific calcium distribution which takes place in myocytes which is responsible for expansion and contraction of myocytes. Various components like

calcium diffusion, pump, leak, source influx and buffers are involved in this calcium signaling in myocytes.

The concentration dependent binding of Ca^{2+} to buffers serves as an indicator of the concentration of free calcium in intracellular measurements. The intracellular binding proteins bind with calcium ion which results into the contraction of cardiac myocytes. The separation of bonded proteins from calcium ion results into the expansion of cardiac myocytes. SERCA pumps transport the Ca^{2+} against its electro chemical gradient. Leak receives the Ca^{2+} that comes from the sarcolema reticulum (SR).Within the SR Ca^{2+} maintains the high capacity and low efficiency of Ca^{2+} binding proteins. They maintain the balances of Ca^{2+} ions through active and passive process. [Bhargava and Pardasani, 2011; Smith, Keizer et. al. 1998] Attempts are reported in the literature for the study of calcium regulation in neuron cell, astrocyte cell, fibroblast cell, oocyte cell etc. [Bhargava and Pardasani, 2011; Jha and Adlakha, 2014; Jha, Adlakha and Mehta, 2014; Kotwani, Adlakha and Mehta, 2013; Panday and Pardasani, 2013; Panday and Pardasani, 2014; Tewari and Pardansi, 2010; Tewari and Pardansi, 2013; Tewari and Pardansi, 2008; Tripathi and Adlakha, 2011] But very few attempts are reported in literature for the study of calcium distribution in myocytes. [Backx et. al. 1989; Luo and Rudy, 1994; Luo and Rudy, 1994b; Michailova et. al. 2002; Shannon et. al. 2004] Most of studies reported on calcium distribution in myocytes are experimental. [Luo and Rudy, 1994; Luo and Rudy, 1994; Michailova et. al. 2002; Shannon et. al.2004]. But few attempts are reported on the study of the effect of source influx, buffer, leak and pump on calcium distribution in myocytes. [Backx et. al. 1989; Smith et. al. 1998] In the present study a mathematical model, for a two dimensional steady state calcium distribution in cardiac myocytes is developed under excess buffering approximation. The important parameters like buffers, diffusion coefficients, out flux due to SERCA pump and influx due to leak has been incorporated in the model. Finite element method is employed to understand the effect of biophysical parameters and processes on calcium distribution in myocytes.

2. MATHEMATICAL FORMULATION

Considering association reaction between Ca^{2+} and buffer,

$$Ca^{2+} + B \underset{k^-}{\overset{k^+}{\Leftrightarrow}} CaB \qquad (1)$$

In equation (1), B represents free buffer, CaB represents Ca^{2+} bound buffer. $k^+$and k^- are association and dissociation rate constants, respectively. By assuming reaction of calcium with buffer follows mass action kinetics, which gives the change in concentration of calcium, free buffer and calcium bound buffers as the following system of equations [Backx et. al., 1989; Luo and Rudy, 1994a; Luo and Rudy, 1994b]

$$\frac{d\left[Ca^{2+}\right]}{dt} = R + J \qquad (2)$$

$$\frac{d[B]}{dt} = R \tag{3}$$

$$\frac{d[CaB]}{dt} = -R \tag{4}$$

where the common reaction term R, is given by

$$R = -k^{+}\left[Ca^{2+}\right][B] + k^{-}[CaB] \tag{5}$$

and J represents Ca^{2+} influx. Equations (2) to (5) are extended to include multiple buffers and the diffusive movement of free Ca^{2+}, Ca^{2+} bound buffer and Ca^{2+} free buffer. By assuming, Fick's diffusion the system of reaction diffusion equations are written as, [Backx et. al., 1989]

$$\frac{\partial\left[Ca^{2+}\right]}{\partial t} = D_{Ca}\nabla^{2}\left[Ca^{2+}\right] + \sum_{i} R_i + J \tag{6}$$

$$\frac{\partial[B_i]}{\partial t} = D_{B_i}\nabla^{2}[B_i] + R_i \tag{7}$$

$$\frac{\partial[CaB_i]}{\partial t} = D_{CaB_i}\nabla^{2}[CaB_i] - R_i \tag{8}$$

where the reaction term, R_i is given by

$$R_i = -k_i^{+}\left[Ca^{2+}\right][B_i] + k_i^{-}[CaB_i] \tag{9}$$

Here, i is an index over Ca^{2+} buffers. D_{Ca} , D_{B_i} , D_{CaB_i} are diffusion coefficients of free Ca^{2+} , bound calcium and free buffer respectively.

Since Ca^{2+} has a molecular weight that is small in comparison to most Ca^{2+} binding species, the diffusion constant of each mobile buffer is not affected by the binding of Ca^{2+} that is $D_{B_i} = D_{CaB_i} = D_i$. [Backx et. al., 1989] Substituting this in equation (7) and (8) and on summation it gives

$$\begin{aligned}\frac{\partial[B_i]_T}{\partial t} &= \frac{\partial[CaB_i]}{\partial t} + \frac{\partial[B_i]}{\partial t} \\ &= D_i\nabla^{2}[CaB_i] + D_i\nabla^{2}[B_i] \\ &= D_i\nabla^{2}[B_i]_T\end{aligned} \tag{10}$$

And

$$R_i = -k_i^+ \left[Ca^{2+}\right]\left[B_i\right] + k_i^- \left(\left[B_i\right]_T - \left[B_i\right]\right) \qquad (11)$$

where

$$\left[B_i\right]_T = \left[CaB_i\right] + \left[B_i\right] \qquad (12)$$

Thus, $[B_i]_T$ remains uniform for all times. (Bhargava and Pardasani, 2011; Tripathi and Adlakha, 2011) Thus, the following equations are obtained for the diffusion of Ca^{2+},

$$\frac{\partial\left[Ca^{2+}\right]}{\partial t} = D_{Ca}\nabla^2\left[Ca^{2+}\right] + \sum_i R_i + J \qquad (13)$$

$$\frac{\partial\left[B_i\right]}{\partial t} = D_i\nabla^2\left[B_i\right] + R_i \qquad (14)$$

where

$$R_i = -k_i^+ \left[Ca^{2+}\right]\left[B_i\right] + k_i^- \left(\left[B_i\right]_T - \left[B_i\right]\right) \qquad (15)$$

In the excess buffer approximation (EBA), equations (6) to (8) are simplified by assuming that the concentration of free Ca^{2+}buffer $[B_i]$, is high enough such that its loss is negligible. [Bhargava and Pardasani, 2011; Tripathi and Adlakha, 2011]

The association and dissociation rate constants for the bimolecular association reaction between Ca^{2+} and buffer can be combined to obtain a dissociation constant, K_i.

$$K_i = k_i^- / k_i^+ \qquad (16)$$

The concentration of Ca^{2+} is necessary to cause 50% of the buffer to be in Ca^{2+} bound form. To show this consider the steady state of equations (6) to (8) in the absence of influx (J=0). Setting the left hand sides of equation (7) and (8) to zero gives [Bhargava and Pardasani, 2011; Tripathi and Adlakha, 2011]

$$\left[B_i\right]_\infty = \frac{K_i\left[B_i\right]_T}{K_i + \left[Ca^{2+}\right]_\infty} \qquad (17)$$

and

$$\left[CaB_i\right]_\infty = \frac{\left[Ca^{2+}\right]_\infty\left[B_i\right]_T}{K_i + \left[Ca^{2+}\right]_\infty} \qquad (18)$$

where $[Ca^{2+}]_\infty$ is the "background". And $[B_i]_\infty$ and $[CaB_i]_\infty$ are the equilibrium concentrations of free and bound buffer with respect to index i. In these expression K_i is the dissociation rate constant of buffer i. Note that higher values for K_i imply that the buffer has a lower affinity for Ca^{2+} and is less easily saturated. In this case, the

equation for the diffusion of Ca^{2+} becomes,

$$\frac{\partial\left[Ca^{2+}\right]}{\partial t} = D_{Ca}\nabla^2\left[Ca^{2+}\right] - \sum_i k_i^+\left[B_i\right]_\infty\left(\left[Ca^{2+}\right]-\left[Ca^{2+}\right]_\infty\right)+J \quad (19)$$

Incorporating out flux J_{pump} due to SERCA pump and in flux J_{leak} due to leak in equation for two dimensional steady state case the equation (19) in polar cylindrical coordinates is given by

$$\frac{1}{r}\frac{\partial}{\partial r}\left(r\frac{\partial\left[Ca^{2+}\right]}{\partial r}\right)+\frac{1}{r^2}\frac{\partial^2\left[Ca^{2+}\right]}{\partial\theta^2}- \frac{k^+\left[B\right]_\infty}{D_{Ca}}\left(\left[Ca^{2+}\right]-\left[Ca^{2+}\right]_\infty\right) + \frac{1}{D_{Ca}}\left(J_{leak}-J_{pump}\right)=0 \quad (20)$$

where

$J_{leak} = V_{leak}\left([Ca^{2+}]_{SR}-[Ca^{2+}]\right)$ *and*

$$J_{pump} = V_{pump}\frac{[Ca^{2+}]^2}{\left(K_{pump}{}^2+[Ca^{2+}]^2\right)}$$

Here V_{leak}, V_{pump} and K_{pump} represents leak rate, serca pump rate and dissociation rate of serca pump respectively. [Smith et.al., 1998]

To solve reaction diffusion equation (20) of calcium concentration appropriate boundary conditions must be supplied. The reasonable boundary condition for this simulation is uniform background Ca^{2+} profile of $[Ca^{2+}]_\infty = 0.1\ \mu M$. It is required that buffer far from the source to remain in equilibrium with Ca^{2+} at all times. Thus the boundary condition on the boundary away from the source is given by [Bhargava and Pardasani, 2011; Tripathi and Adlakha, 2011; Jha, Adlakha and Mehta, 2014]

$$\lim_{r\to\infty,\theta\to 0}\left[Ca^{2+}\right]=\left[Ca^{2+}\right]_\infty \quad (21)$$

At the source, it is assumed that influx takes place and therefore the boundary condition is expressed as, [Bhargava and Pardasani, 2011; Tripathi and Adlakha, 2011; Jha, Adlakha and Mehta, 2014]

$$\lim_{r\to\infty,\theta\to\pi}\left(-2\pi D_{Ca}r\frac{\partial\left[Ca^{2+}\right]}{\partial r}\right)=\sigma_{Ca} \quad (22)$$

We define an influx of free Ca^{2+} at the rate σ_{Ca} by Faraday's law, $\sigma_{Ca} = \frac{I_{Ca}}{zF}$ where I_{Ca} is amplitude of element of Ca^{2+} release, F is Faraday's constant and Z is valence of Ca^{2+} ion. [Bhargava and Pardasani, 2011; Luo and Rudy, 1994; Luo and Rudy, 1994]. Hence, the problem reduces to find the solution of equation (20) with respect to the boundary conditions (21) and (22).

Here, $\left[Ca^{2+}\right]_{\infty}$ is the background calcium concentration, $\left[B\right]_{\infty}$ is the total buffer concentration, σ_{Ca} represents the flux. $\left[Ca^{2+}\right]$ approaches to the background concentration 0.1 μM as r tends to ∞ and θ tends to π. But the domain taken here is not infinite but finite one. Here, the distance required for $\left[Ca^{2+}\right]$ to attain background concentration is 7.8 μm for the Cardiac Myocytes (i.e. radius of the Cardiac Myocytes). [Michailova et. al., 2002]

The study is performed for two cases as given below:

Case I: When $K_{pump} >> [Ca^{2+}]$ then we have [Bhargava and Pardasani, 2011; Tripathi and Adlakha, 2011] $\frac{\left[Ca^{2+}\right]^2}{K^2_{pump} + \left[Ca^{2+}\right]^2} \le \frac{\left[Ca^{2+}\right]^2}{K^2_{pump}} \le \frac{\left[Ca^{2+}\right]}{K_{pump}}$ (a)

In view of above equation (20) is taken as:

$$\frac{1}{r}\frac{\partial}{\partial r}\left(r\frac{\partial\left[Ca^{2+}\right]}{\partial r}\right)+\frac{1}{r^2}\frac{\partial^2\left[Ca^{2+}\right]}{\partial\theta^2}-\frac{k^+[B]_{\infty}}{D_{Ca}}\left(\left[Ca^{2+}\right]-\left[Ca^{2+}\right]_{\infty}\right)$$
$$+\frac{1}{D_{Ca}}\left(J_{leak}-J_{pump}\right)=0 \qquad (23)$$

where

$J_{leak} = V_{leak}\left([Ca^{2+}]_{SR} - [Ca^{2+}]\right)$ *and*

$J_{pump} = V_{pump}\frac{[Ca^{2+}]}{K_{pump}}$

Now the finite element method is employed to solve equation (23) with boundary conditions (21) and (22). The discretized variational integral of equation (23) is given by

$$I^{(e)} = \frac{1}{2}\int_{r_i}^{r_j}\int_{\theta_i}^{\theta_k}\left[\left(\left(r\frac{\partial u^{(e)}}{\partial r}\right)^2+\left(\frac{\partial u^{(e)}}{\partial\theta}\right)^2\right)\right]drd\theta +$$
$$\frac{1}{2}\int_{r_i}^{r_j}\int_{\theta_i}^{\theta_k}\left[\frac{k^+[B]_{\infty}}{D_{Ca}}r^2u^{(e)2}-\frac{2k^+[B]_{\infty}}{D_{Ca}}u_{\infty}u^{(e)}r^2\right]drd\theta$$
$$-\frac{1}{2}\int_{r_i}^{r_j}\int_{\theta_i}^{\theta_k}\left[\frac{r^2V_{leak}}{D_{Ca}}\left(2u^{(e)}u_{SR}-u^{(e)^2}\right)-\frac{V_{pump}r^2}{K_{pump}D_{Ca}}\right]drd\theta$$
$$-\int_{\theta_i}^{\theta_k}\left[\frac{\sigma_{Ca}}{2\pi D_{Ca}}u^{(e)}\right]d\theta \qquad (24)$$

Here, 'u' is used in lieu of $\left[Ca^{2+}\right]$, e = 1, 2,…N.

Case II: When $K_{pump} << [Ca^{2+}]$ then we assume $K_{pump} = \alpha\left[Ca^{2+}\right]$ $for\, 0 \le \alpha \le 1$, [Bhargava and Pardasani, 2011; Tripathi and Adlakha, 2011]

$$\frac{\left[Ca^{2+}\right]^2}{K^2{}_{pump} + \left[Ca^{2+}\right]^2} = \frac{1}{\alpha^2 + 1} \qquad (b)$$

In view of above equation (20) is taken as:

$$\frac{1}{r}\frac{\partial}{\partial r}\left(r\frac{\partial\left[Ca^{2+}\right]}{\partial r}\right) + \frac{1}{r^2}\frac{\partial^2\left[Ca^{2+}\right]}{\partial\theta^2} - \frac{k^+[B]_\infty}{D_{Ca}}\left(\left[Ca^{2+}\right] - \left[Ca^{2+}\right]_\infty\right) + \frac{1}{D_{Ca}}\left(J_{leak} - J_{pump}\right) = 0 \qquad (25)$$

$where$

$$J_{leak} = V_{leak}\left([Ca^{2+}]_{SR} - [Ca^{2+}]\right)\ and$$

$$J_{pump} = \frac{V_{pump}}{\alpha^2 + 1}$$

Now the finite element method is employed to solve equation (25) with boundary conditions (21) and (22). The discretized variational integral of equation (25) is given by

$$I^{(e)} = \frac{1}{2}\int_{r_i}^{r_j}\int_{\theta_i}^{\theta_k}\left[\left(\left(r\frac{\partial u^{(e)}}{\partial r}\right)^2 + \left(\frac{\partial u^{(e)}}{\partial\theta}\right)^2\right)\right]drd\theta + \frac{1}{2}\int_{r_i}^{r_j}\int_{\theta_i}^{\theta_k}\left[\frac{k^+[B]_\infty}{D_{Ca}}r^2u^{(e)2} - \frac{2k^+[B]_\infty}{D_{Ca}}u_\infty u^{(e)}r^2\right]drd\theta - \frac{1}{2}\int_{r_i}^{r_j}\int_{\theta_i}^{\theta_k}\left[\frac{r^2V_{leak}}{D_{Ca}}\left(2u^{(e)}u_{SR} - u^{(e)^2}\right) - \frac{r^2V_{pump}u^{(e)}}{D_{Ca}}\right]drd\theta - \int_{\theta_i}^{\theta_k}\left[\frac{\sigma_{Ca}}{2\pi D_{Ca}}u^{(e)}\right]d\theta \qquad (26)$$

Here, 'u' is used in lieu of $\left[Ca^{2+}\right]$, e = 1, 2,…N.

Assuming that the cardiac myocytes is of circular shape and it is divided into coaxial circular sectional elements , given in Fig 1

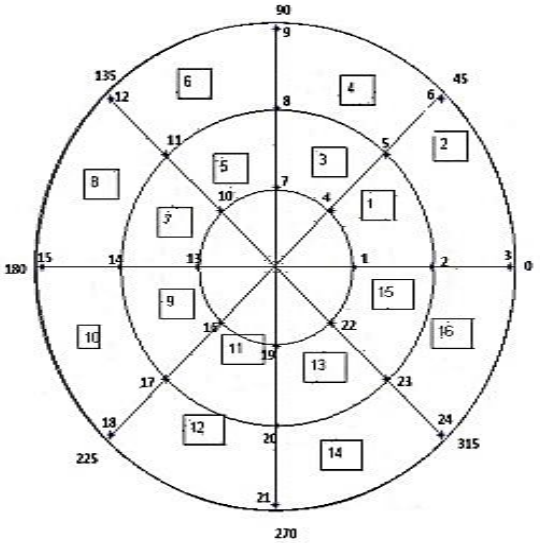

Fig 1: Finite element Discretization of myocyte

Here the number in square represents the number of elements and number without square represents the nodal points where the nodal point 15 represents point source of calcium. The Table 1 represents the element information.

Table 1: Element information

element	a	b	c	d
1	1	2	4	5
2	2	3	5	6
3	4	5	7	8
4	5	6	8	9
5	7	8	10	11
6	8	9	11	12
7	10	11	13	14
8	11	12	14	15
9	13	14	16	17
10	14	15	17	18
11	16	17	19	20
12	17	18	20	21
13	19	20	22	23
14	20	21	23	24
15	22	23	1	2
16	23	24	2	3

The thickness of each element is very small, therefore $u^{(e)}$ is assigned bilinear variation with respect to position. The following bilinear shape function for the calcium concentration within each element has been employed.

$$u^{(e)} = a_1^{(e)} + a_2^{(e)} r + a_3^{(e)} \theta + a_4^{(e)} r\theta \quad (27)$$

In matrix form the equation (27) can be written as

$$u^{(e)} = P^T A^{(e)} \quad (28)$$

where

$$P^T = \begin{bmatrix} 1 & r & \theta & r\theta \end{bmatrix} \text{ and } A^{(e)} = \begin{bmatrix} a_1^{(e)} \\ a_2^{(e)} \\ a_3^{(e)} \\ a_4^{(e)} \end{bmatrix}$$

Also

$$u_i^{(e)} = a_1^{(e)} + a_2^{(e)} r_i + a_3^{(e)} \theta_i + a_4^{(e)} r_i \theta_i \quad (29)$$

$$u_j^{(e)} = a_1^{(e)} + a_2^{(e)} r_j + a_3^{(e)} \theta_j + a_4^{(e)} r_j \theta_j \quad (30)$$

$$u_k^{(e)} = a_1^{(e)} + a_2^{(e)} r_k + a_3^{(e)} \theta_k + a_4^{(e)} r_k \theta_k \quad (31)$$

$$u_l^{(e)} = a_1^{(e)} + a_2^{(e)} r_l + a_3^{(e)} \theta_l + a_4^{(e)} r_l \theta_l \quad (32)$$

Using equations (29)-(32) we get

$$\overline{u}^{(e)} = P^{(e)} A^{(e)} \quad (33)$$

where

$$P^{(e)} = \begin{bmatrix} 1 & r_i & \theta_i & r_i\theta_i \\ 1 & r_j & \theta_j & r_j\theta_j \\ 1 & r_k & \theta_k & r_k\theta_k \\ 1 & r_l & \theta_l & r_l\theta_l \end{bmatrix} \text{ and } \overline{u}^{(e)} = \begin{bmatrix} u_i^{(e)} \\ u_j^{(e)} \\ u_k^{(e)} \\ u_l^{(e)} \end{bmatrix}$$

From Equation (28) and (33) we get

$$u^{(e)} = P^T R^{(e)} \overline{u}^{(e)} \quad (34)$$

where $R^{(e)} = P^{(e)-1}$

Now the integrals given in equations (24) and (26) in matrix notation can also be written as,

$$
\begin{aligned}
I^{(e)} = & \frac{1}{2}\int_{r_i}^{r_j}\int_{\theta_i}^{\theta_k}\left[\left(r\,\mathrm{P_r}^{T}\,R^{(e)}\overline{u}^{(e)}\right)^2\right]drd\theta + \\
& \frac{1}{2}\int_{r_i}^{r_j}\int_{\theta_i}^{\theta_k}\left[\left(P_\theta^{T}R^{(e)}\overline{u}^{(e)}\right)^2\right]drd\theta + \\
& \frac{1}{2}\int_{r_i}^{r_j}\int_{\theta_i}^{\theta_k}\left[\frac{k^{+}[B]_\infty}{D_{Ca}}r^2\left(\mathrm{P}^{T}\,R^{(e)}\overline{u}^{(e)}\right)^2\right]drd\theta \\
& -\frac{1}{2}\int_{r_i}^{r_j}\int_{\theta_i}^{\theta_k}\left[\frac{2k^{+}[B]_\infty}{D_{Ca}}u_\infty r^2\left(\mathrm{P}^{T}\,R^{(e)}\overline{u}^{(e)}\right)\right]drd\theta \\
& -\frac{1}{2}\int_{r_i}^{r_j}\int_{\theta_i}^{\theta_k}\left[\frac{r^2V_{leak}}{D_{Ca}}\left(2u_{SR}\,\mathrm{P}^{T}\,R^{(e)}\overline{u}^{(e)}\right)\right]drd\theta \\
& +\frac{1}{2}\int_{r_i}^{r_j}\int_{\theta_i}^{\theta_k}\left[\frac{r^2V_{leak}}{D_{Ca}}\left(\left(\mathrm{P}^{T}\,R^{(e)}\overline{u}^{(e)}\right)^2\right)\right]drd\theta \\
& +\frac{1}{2}\int_{r_i}^{r_j}\int_{\theta_i}^{\theta_k}\left[\frac{r^2V_{pump}}{K_{pump}D_{Ca}}\left(\mathrm{P}^{T}\,R^{(e)}\overline{u}^{(e)}\right)^2\right]drd\theta \\
& -\int_{\theta_i}^{\theta_k}\left[\frac{\sigma_{Ca}}{2\pi D_{Ca}}\overline{u}^{(e)}\right]d\theta
\end{aligned}
\tag{35}
$$

and

$$
\begin{aligned}
I^{(e)} = & \frac{1}{2}\int_{r_i}^{r_j}\int_{\theta_i}^{\theta_k}\left[\left(r\,\mathrm{P_r}^{T}\,R^{(e)}\overline{u}^{(e)}\right)^2\right]drd\theta \\
& +\frac{1}{2}\int_{r_i}^{r_j}\int_{\theta_i}^{\theta_k}\left[\left(P_\theta^{T}R^{(e)}\overline{u}^{(e)}\right)^2\right]drd\theta \\
& +\frac{1}{2}\int_{r_i}^{r_j}\int_{\theta_i}^{\theta_k}\left[\frac{k^{+}[B]_\infty}{D_{Ca}}r^2\left(\mathrm{P}^{T}\,R^{(e)}\overline{u}^{(e)}\right)^2\right]drd\theta \\
& -\frac{1}{2}\int_{r_i}^{r_j}\int_{\theta_i}^{\theta_k}\left[\frac{2k^{+}[B]_\infty}{D_{Ca}}u_\infty r^2\left(\mathrm{P}^{T}\,R^{(e)}\overline{u}^{(e)}\right)\right]drd\theta \\
& -\frac{1}{2}\int_{r_i}^{r_j}\int_{\theta_i}^{\theta_k}\left[\frac{r^2V_{leak}}{D_{Ca}}\left(2u_{SR}\,\mathrm{P}^{T}\,R^{(e)}\overline{u}^{(e)}\right)\right]drd\theta \\
& +\frac{1}{2}\int_{r_i}^{r_j}\int_{\theta_i}^{\theta_k}\left[\frac{r^2V_{leak}}{D_{Ca}}\left(\left(\mathrm{P}^{T}\,R^{(e)}\overline{u}^{(e)}\right)^2\right)\right]drd\theta \\
& +\frac{1}{2}\int_{r_i}^{r_j}\int_{\theta_i}^{\theta_k}\left[\frac{r^2V_{pump}}{D_{Ca}}\left(\mathrm{P}^{T}\,R^{(e)}\overline{u}^{(e)}\right)\right]drd\theta \\
& -\int_{\theta_i}^{\theta_k}\left[\frac{\sigma_{Ca}}{2\pi D_{Ca}}\overline{u}^{(e)}\right]d\theta
\end{aligned}
\tag{36}
$$

Now $I^{(e)}$ is minimized with respect to $\bar{u}^{(e)}$, $\frac{dI^{(e)}}{d\bar{u}^{(e)}} = 0$,

$$\bar{u}^{(e)} = \begin{bmatrix} u_i & u_j & u_k & u_l \end{bmatrix}^T, e = (1,2,...16)$$

$$\frac{dI}{d\bar{u}^{(e)}} = \sum_{e=1}^{N} \bar{M}^{(e)} \frac{dI^{(e)}}{d\bar{u}^{(e)}} \bar{M}^{(e)T}$$

$$\bar{M}^{(e)} = \begin{bmatrix} 0 & 0 & 0 & 0 \\ 1 & 0 & 0 & 0 \\ 0 & 1 & 0 & 0 \\ 0 & 0 & 1 & 0 \\ 0 & 0 & 0 & 1 \\ \bullet & \bullet & \bullet & \bullet \\ 0 & 0 & 0 & 0 \end{bmatrix}_{(24\times4)} \begin{matrix} \\ (i^{th}\ row) \\ (j^{th}\ row) \\ (k^{th}\ row) \\ (l^{th}\ row) \\ \\ \end{matrix} \quad and\ I = \sum_{e=1}^{16} I^{(e)}$$

This leads to following system of linear algebraic equations

$$[K]_{(24\times24)}[\bar{u}]_{(24\times1)} = [F]_{(24\times1)} \qquad (37)$$

Here, $\bar{u} = \begin{bmatrix} u_1 & u_2 & \bullet & \bullet & \bullet & u_{24} \end{bmatrix}^T$, K is characteristic matrix and F is characteristic vector.

Gaussian Elimination method is employed to solve the system (37).

3. RESULTS AND DISCUSSION

A computer program in MATLAB 7.10.0.499 is developed to find numerical solution to the entire problem. To find the solution of equation (37) the biophysical parameters are taken from the literature as given in Table 2. [Michailova et. al., 2002]

Table 2: Biophysical parameters. [Michailova et. al., 2002]

R	Radius of the cell	7.8 μm
I_{Ca}	Amplitude of elemental Ca^{2+} release	1 p A
F	Faraday's constant	96500 C/mol
Z	Valence of Ca^{2+} ion	2
D_{Ca}	Diffusion coefficient of free Ca^{2+} in cytosol	780 $\mu m^2 / s$
$[B_i]_T$	Total concentration for each Ca^{2+} buffer (Troponin C)	70 μM
K_i	Dissociation constant (Troponin C) $= \frac{k_i^-}{k_i^+}$,	0.51 μM
$[Ca]_\infty$	Intracellular free Ca^{2+} concentration at rest	0.1 μM
V_{pump}	SERCA pump rate	400 $\mu M^{-1} S^{-1}$
V_{leak}	Leak rate	0.02 $\mu M^{-1} S^{-1}$
K_{pump}	Dissociation rate of SERCA pump	0.2 μM

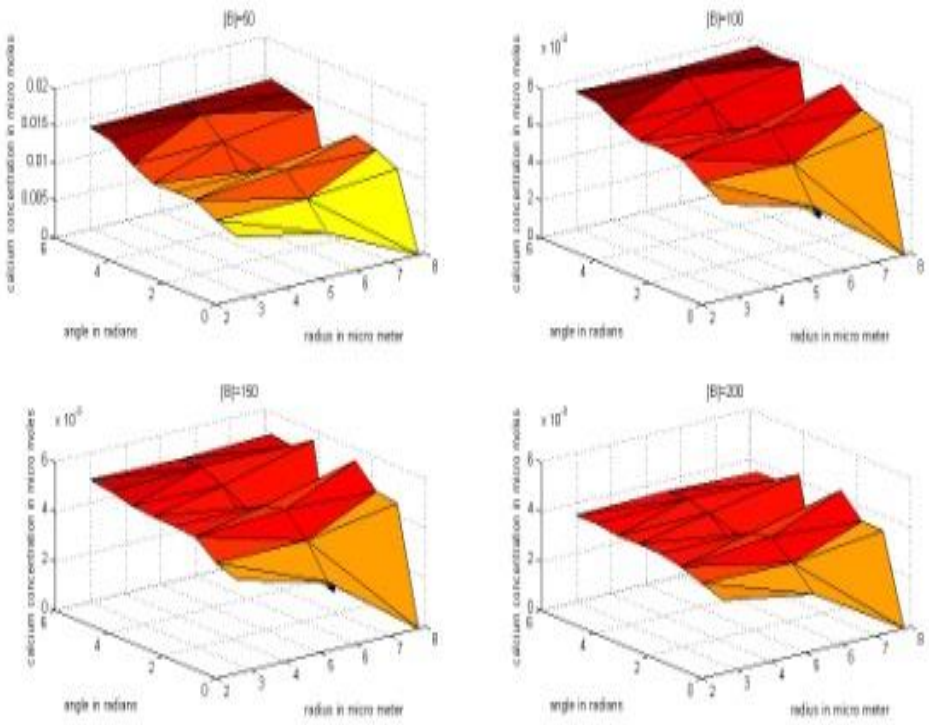

Fig 2: Difference of calcium concentration in myocyte cell with and without pump in absence of leak for Case I at different buffer concentrations

Fig 2 represents the difference of $[Ca^{2+}]$ in myocyte cell with and without pump in absence of leak for case I at different buffer concentrations 50 μM, 100 μM, 150 μM and 200 μM. In Fig 2, it is observed that the difference in $[Ca^{2+}]$ is zero at source, increases initially along r and θ direction as we move away from the source and finally becomes zero at r = 7.8 μM and θ = 0. The difference in $[Ca^{2+}]$ is maximum for buffer concentration 50 μM and minimum for buffer concentration 200 μM. This difference in $[Ca^{2+}]$ decreases in the ratio of increase in buffer concentration. The effect of pump at higher buffer concentration is not significant.

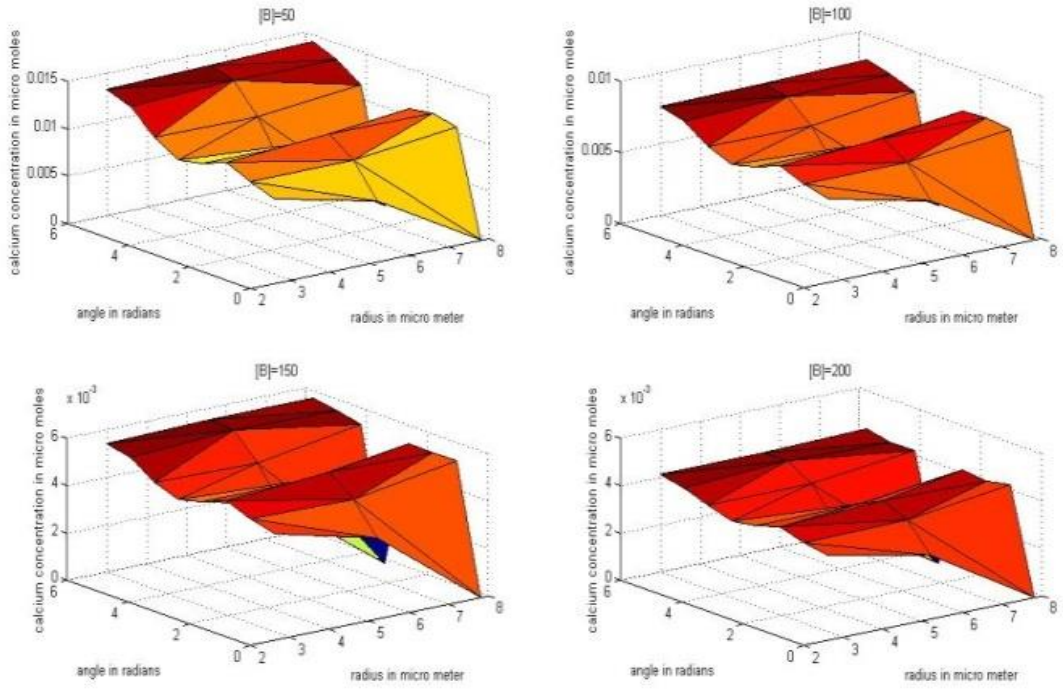

Fig 3 Difference of calcium concentration in myocyte cell with and without leak in absence of pump at different buffer concentrations

Fig 3 represents the difference of $[Ca^{2+}]$ in myocyte cell with and without leak in absence of pump at buffer concentrations 50 μM, 100 μM, 150 μM and 200 μM. In Fig 3, it is observed that the difference in $[Ca^{2+}]$is zero at source, increases initially along r and θ direction as we move away from the source and finally becomes zero at r = 7.8 μM and θ = 0. The difference in $[Ca^{2+}]$ is maximum for buffer concentration 50 μM and minimum for buffer concentration 200 μM. This difference in $[Ca^{2+}]$ decreases in the ratio of increase in buffer concentration. The effect of leak at higher buffer concentration is not significant due to buffering process.

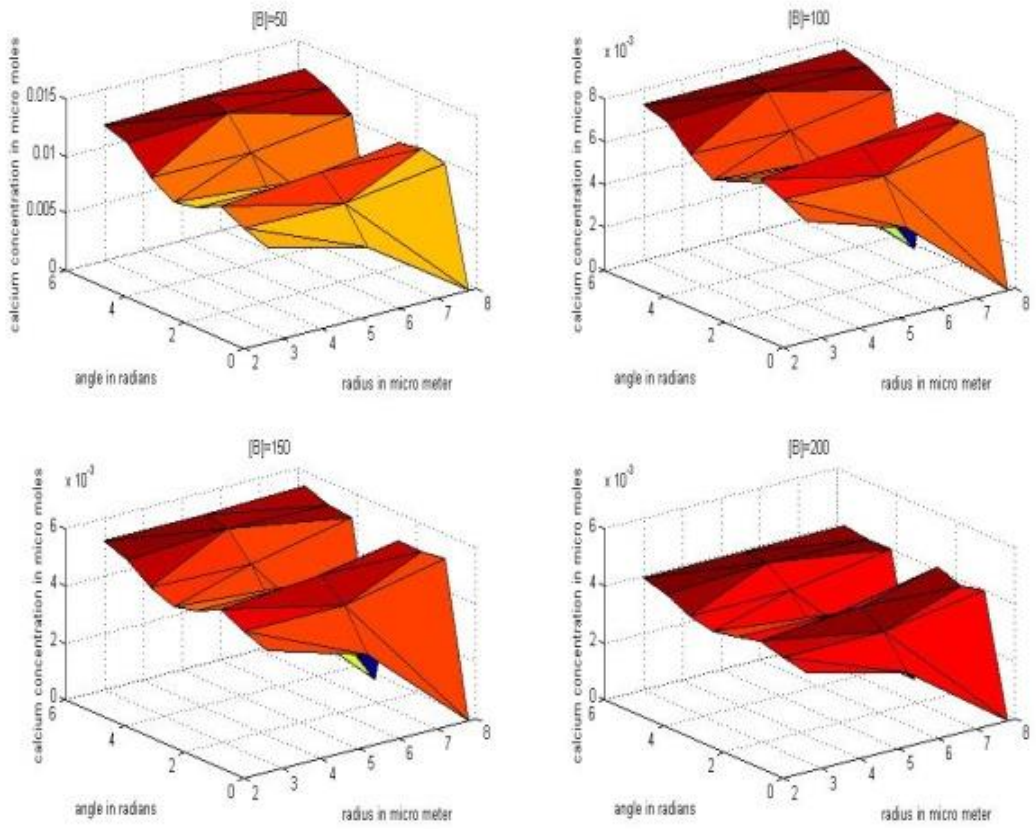

Fig 4: Difference of calcium concentration in myocyte cell with and without leak in presence of pump for case I at different buffer concentrations

Fig 4 represents the difference of $[Ca^{2+}]$ in myocyte cell with and without leak in presence of pump for case I at buffer concentrations 50 μM, 100 μM, 150 μM and 200 μM. In Fig 4, it is observed that the difference in $[Ca^{2+}]$ is zero at source, increases initially along r and θ direction as we move away from the source and finally becomes zero at r = 7.8 μM and θ = 0. The difference in $[Ca^{2+}]$ is maximum for buffer concentration 50 μM and minimum for buffer concentration 200 μM. This difference in $[Ca^{2+}]$ decreases in the ratio of increase in buffer concentration. In Fig 4 the effect of leak on calcium distribution in myocyte cell is not clearly visible as it is balanced by the presence of pump and buffer compared to Fig 3.

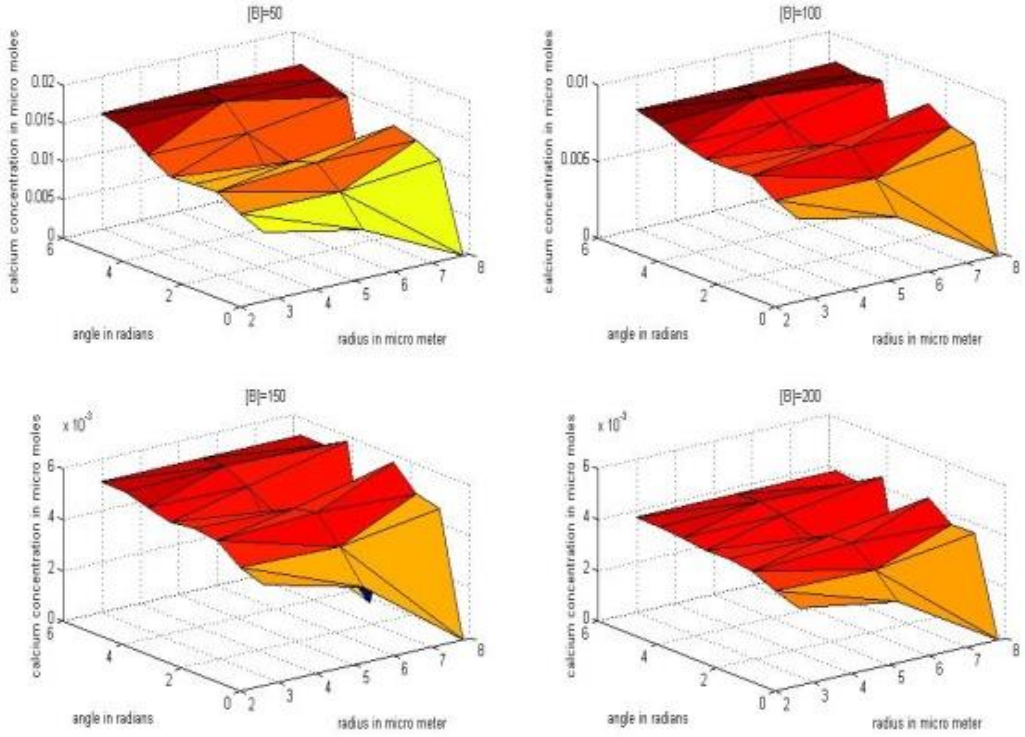

Fig 5 Difference of calcium concentration in myocyte cell with and without pump in presence of leak for case I at different buffer concentrations.

Fig 5 represents the difference of $[Ca^{2+}]$ in myocyte cell with and without pump in presence of leak for case I at buffer concentrations 50 μM, 100 μM, 150 μM and 200 μM. In Fig 5, it is observed that the difference in $[Ca^{2+}]$ is zero at source, increases initially along r and θ direction as we move away from the source and finally becomes zero at r = 7.8 μM and θ = 0. The difference in calcium concentration is maximum for buffer concentration 50 μM and minimum for buffer concentration 200 μM. This difference in $[Ca^{2+}]$ decreases in the ratio of increase in buffer concentration. In Fig 4 the effect of pump on calcium distribution in myocyte cell is not clearly visible as it is balanced by influx due to leak. Comparing Fig 5 with Fig 2 we observe that the difference in $[Ca^{2+}]$ in Fig 5 is higher than that Fig 2 for the corresponding values of buffer concentrations. This is due to the presence of leak in case of Fig 5 and absence of leak in case of Fig 2.

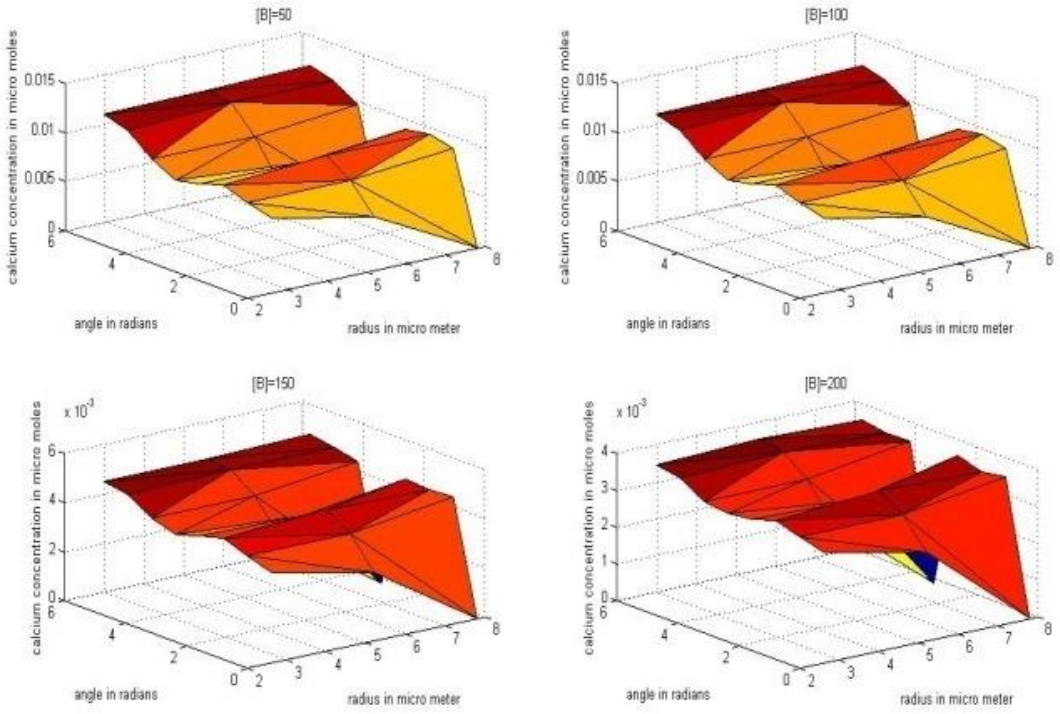

Fig 6: Difference of calcium concentration in myocyte cell with and without pump in absence of leak for Case II at different buffer concentration

Fig 6 represents the difference of $[Ca^{2+}]$ in myocyte cell with and without pump in absence of leak for case II at different buffer concentrations 50 μM, 100 μM, 150 μM and 200 μM. In Fig 6, it is observed that the difference in $[Ca^{2+}]$ is zero at source, increases initially along r and θ direction as we move away from the source and finally becomes zero at r = 7.8 μM and θ = 0. The difference in calcium concentration is maximum for buffer concentration 50 μM and minimum for buffer concentration 200 μM. This difference in $[Ca^{2+}]$ decreases in the ratio of increase in buffer concentration. The effect of pump at higher buffer concentration is not significant in absence of leak due to the buffer. It is also observed that in case II (Fig 6) the difference in $[Ca^{2+}]$ is higher than that of case I (Fig 2) at lower buffer concentration. The effect of pump is dominated by the higher buffer concentration in both cases I and II.

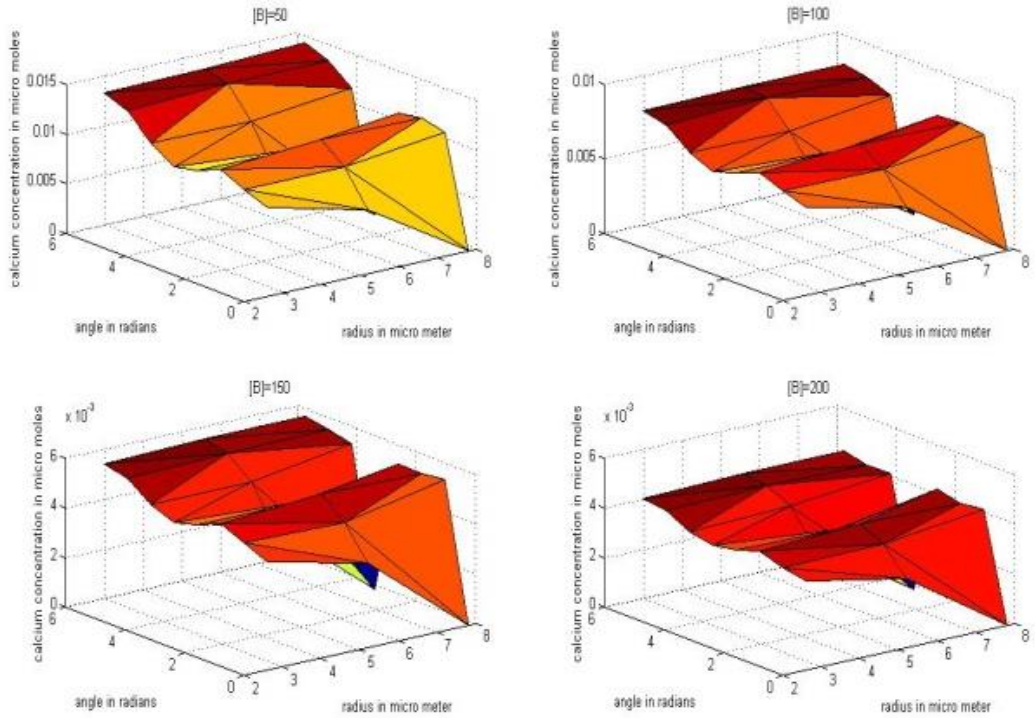

Fig 7: Difference of calcium concentration in myocyte cell with and without leak in presence of pump for case II at different buffer concentrations

Fig 7 represents the difference of $[Ca^{2+}]$ in myocyte cell with and without leak in presence of pump for case II at buffer concentrations 50 μM, 100 μM, 150 μM and 200 μM. In Fig 7, it is observed that the difference in $[Ca^{2+}]$ is zero at source, increases initially along r and θ direction as we move away from the source and finally becomes zero at r = 7.8 μM and θ = 0. The difference in calcium concentration is maximum for buffer concentration 50 μM and minimum for buffer concentration 200 μM. This difference in $[Ca^{2+}]$ decreases in the ratio of increase in buffer concentration. In Fig 7 the effect of leak on calcium distribution in myocyte cell is not clearly visible as it is balanced by the presence of pump and buffer compared to Fig 3. It is also observed that in Fig 7 for case II the difference in $[Ca^{2+}]$ is higher than that in Fig 4 for case I at lower buffer concentration. This is due to the smaller value of dissociation rate constant of SERCA pump for case in Fig 7. At higher values of buffer concentration the effect of pump and leak is balanced by the buffers.

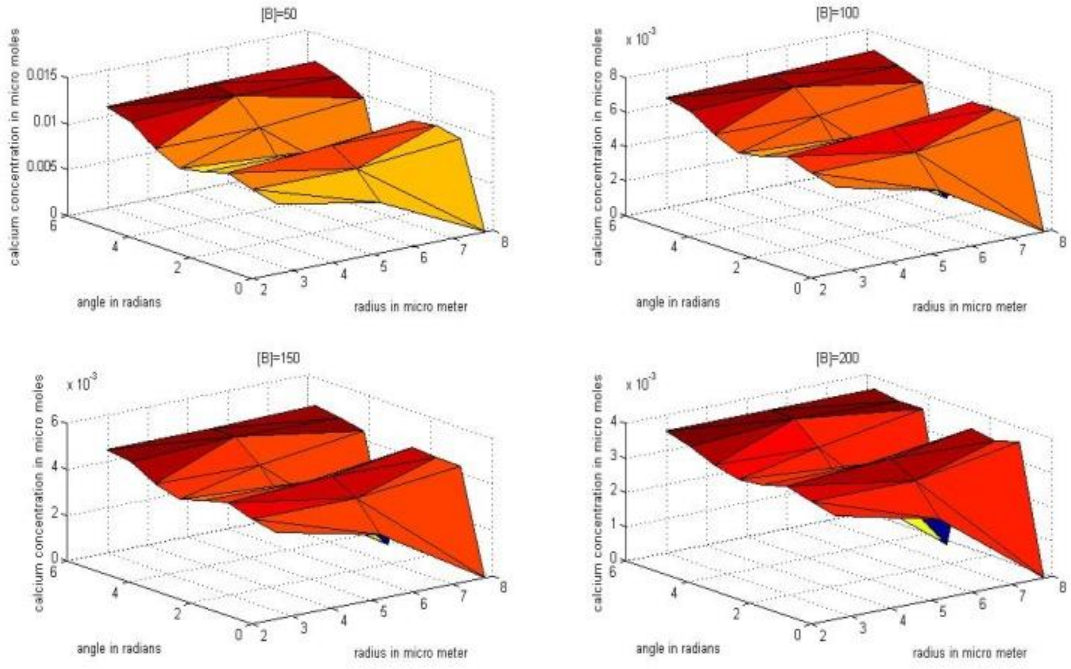

Fig 8. Difference of calcium concentration with and without pump in presence of leak for case II at different buffer concentrations

Fig 8 represents the difference of $[Ca^{2+}]$ in myocyte cell with and without pump in presence of leak for case I at buffer concentrations 50 μM, 100 μM, 150 μM and 200 μM. In Fig 8, it is observed that the difference in $[Ca^{2+}]$ is zero at source, increases initially along r and θ direction as we move away from the source and finally becomes zero at r = 7.8 μM and θ = 0. The difference in $[Ca^{2+}]$ is maximum for buffer concentration 50 μM and minimum for buffer concentration 200 μM. This difference in $[Ca^{2+}]$ decreases in the ratio of increase in buffer concentration. In Fig 8 the effect of leak on calcium distribution in myocyte cell is not clearly visible as it is balanced by influx due to leak. It is also observed that in Fig 8 for case II the difference in $[Ca^{2+}]$ is higher than that in Fig 5 for case I at lower buffer concentration. This is due to the smaller value of dissociation rate constant of SERCA pump for case in Fig 8.

4. CONCLUSION

A two dimensional finite element simulation is proposed to understand the calcium regulation mechanism in a myocyte cell involving excess buffers, pump and leak. The proposed work has proved to be effective in generating interesting results. On the basis of the results it can be concluded that the pump, buffers and leak have significant effect on calcium distribution in a myocyte cell. The effect of pump and leak on $[Ca^{2+}]$ in a

myocyte cell is more significant at lower buffer concentrations. This happen in the case where buffers have got saturated and their capacity to bind calcium has become low. But when buffer concentration is high, then it dominates over the effect of pump and leak in regulating the $[Ca^{2+}]$ in a myocyte cell. In the entire myocyte cell exhibits a beautiful coordinated mechanism to regulate the calcium concentration in the cell. The results give us better insights of theses mechanisms in the cell. Such finite element models can be developed to study the calcium distribution in myocytes in different clinical situations. The information generated from such models can be of great use to biomedical scientists for developing protocols for diagnosis and treatment of heart diseases.

5. REFERENCES

[1] Backx, P. H., De Tonb, P. P., Jurjen, H. K. ,Van Deen, Barbara J. M., Mulder, and Henke, D. J., "A Model of Propagating Calcium-induced Calcium Release Mediated by Calcium diffusion", The Journal of General Physiology, 93: 963-977, 1989.

[2] Bhargava, N. and Pardasani, K. R., "Galerkin Approximation for the Problem of Calcium Diffusion in Neuron Cell Involving Pump, Leak and Excess Buffering Approximation", Applied Mathematical Science, 5(55):2707-2720,2011.

[3] Jha, A and Adlakha, N., "Finite element model to study the effect of exogenous buffer on calcium dynamics in dendritic spines", International Journal of Modeling, Simulation and Scientific Computation, 5(2): 1350027(1-12), 2014.

[4] Jha, B K, Adlakha, N and Mehta, M. N., "Two dimensional finite element model to study calcium distribution in Astrocytes in presence of excess buffer", International Journal of Biomathematics, 7(3):1-11, 2014.

[5] Jha, B. K., Adlakha, N. and Mehta, M. N., "Two-dimensional finite element model to study calcium distribution in astrocytes in presence of VGCC and excess buffer", International Journal of Modeling, Simulation and Scientific Computing, 4(2): 1-15, 2013.

[6] Kotwani, M., Adlakha, N. and Mehta, M. N., "Finite Element Model to Study the Effect of Buffers, Source Amplitude and Source Geometry on Spatio-Temporal Calcium Distribution in Fibroblast Cell", Journal of Medical Imaging and Health Informatics, 4(6):840-847, 2014.

[7] Luo and Rudy, "A Dynamic Model of the Cardiac Ventricular Action Potential. I Simulations of Ionic Currents and Concentration Changes", Circular Research, 4: 1071-1096, 1994.

[8] Luo and Rudy, "A Dynamic model of the Cardiac Ventricular action potential. II After depolarization, triggered activity, and potentiation", Circular Research, 74: 1097-1113, 1994.

[9] Michailova, A., Del, F., Egger, M. and Niggli, E., "Spatiotemporal Features of Ca^{2+} Buffering and Diffusion in Atrial Cardiac Myocytes with inhibited Sarcoplasmic Reticulum", Biophysical Journal, 83: 3134-3151, 2002.

[10] Panday, S and Pardasani, K R, "Finite element model to study effect of Advection diffusion and Na^{+}/Ca^{2+} exchanger on calcium distribution in Oocyte", Journal of Medical Imaging and Health information, 3: 374-379, 2013.

[11] Panday, S and Pardasani, K R, "Finite element model to study the mechanics of calcium regulations in Oocyte", Journal of Mechanics in Medicine and Biology, 14(2): 145002(1-16), 2014.

[12] Post, J. and Langer, G., "Sarcolemmal Ca^{2+} binding sites in Heart: I. Molecular origin in gas dissected", Journal of Membrane Biology, 129- 149, 1992.

[13] Shannon, T. R., Wang, F., Puglisi, J., Weber, C. and Bers D. M., "A Mathematical Treatment of Integrated Ca Dynamics within the Ventricular Myocytes", Biophysical Journal, 87:3351-3371, 2004.

[14] Smith, G. D., Keizer, J. E., Stern, M. D., Lederer, W. J. and Cheng H.,"A Simple Numerical Model of Calcium Spark Formation and Detection in Cardiac Myocytes", Biophysical Journal, 75: 15-32, 1998.

[15] Tewari, S and Pardasani, K R, "Finite Element Model to Study Two Dimensional Unsteady State Cytosolic Calcium Diffusion in Presence of Excess Buffers", IAENG Journal of Applied Mathematics, 40(3): 1-5, 2010.

[16] Tewari, S and Pardasani, K R, "Modeling effect of sodium pump on calcium oscillations in neuron cells", Journal of Multiscale Modelling, 4(3): 1250010(1-16), 2013.

[17] Tripathi, A. and Adlakha, N., "Finite Volume Model to Study Calcium Diffusion in Neuron Involving J_{RYR}, J_{SERCA} and J_{LEAK}", Journal of computing, 3(11): 41-47, 2011.